ISSN 1392-1207. MECHANIKA. Vol. 31, No. 5, 2025: 440–454

Predictive Maintenance of Rotating Machines, Application to the DHB Semolina Decorticator

Rabah MAGRAOUI*, Adel ZEMIRLINE, Mohammed OUALI*****

**University of Blida 1, Department of Mechanical Engineering, Faculty of Engineering Sciences, Structural Mechanics Research Laboratory, Mechanical Engineering Department, Blida, Algeria, E-mails: magraoui_rabah@univ-blida.dz, r.magraoui.labstructures.usdb@gmail.com*

***Laboratory of Mechanics Physics and Mathematical Modelling LMPMM, Medea University, Algeria, Structural Mechanics Research Laboratory, Mechanical Engineering Department, Blida, Algeria, E-mails: zemirline.adel@univ-medea.dz, zemirline.adel@yahoo.com (Corresponding Author)*

****University of Blida 1, Department of Mechanical Engineering, Faculty of Engineering Sciences, Structural Mechanics Research Laboratory, Mechanical Engineering Department, Blida, Algeria, E-mails: ouali_mohammed@univ-blida.dz, oualimohammed@yahoo.fr*

https://doi.org/10.5755/j02.mech.36611

1. Introduction

Rotating machines play a crucial role in the field of technology and industry, encompassing mechanical industry, electricity production, air transportation, heating, air conditioning, household appliances. and more.

Failures in rotating machines are diverse, including imbalances, clearances, bearing issues, coupling faults, alignment problems and more. The majority of these failures result in vibrations in the malfunctioning machine. Vibrations serve as indicators of failure symptoms that allow for the interpretation of the mechanical state of a rotating machine. Consequently, these vibrations need to be analyzed through tools for the detection and diagnosis of these failures.

Rotating machines in every factory have the capacity to stop production. Catastrophic failures can occur although some critical machines have vibration protection systems.

Vibration measurements warn of the general state of health of a machine. As faults start to develop, the dynamic behaviour of the machine changes. Manufacturers insist on the reliability and availability of industrial machines. Identifying defects at an early stage, before a failure occurs, is essential.

Machinery Vibration Analysis and Predictive Maintenance provides a detailed examination of the detection, location and diagnosis of faults in rotating and reciprocating machinery using vibration analysis. Vibration analysis aims to identify defects that may arise during the operation of rotating machines. Through appropriate detection or diagnosis, it helps prevent breakdowns and allows for timely intervention, especially during scheduled stops.

The purpose of vibration analysis is to determine the faults that may arise during the operation of the rotating machine. It makes it possible.

through appropriate screening or diagnosis. to avoid breakage and to intervene at the appropriate time and during scheduled shutdowns.

Inevitable defects in rotating machines are numerous. sometimes stemming from design or manufacturing issues. A practical example is the decorticator in a semolina mill. which has experienced frequent unexpected stops since its commissioning due to a design flaw in one of its transmission components. These unplanned stops have led to financial losses in terms of production and product quality. Hence. a study of this system was undertaken to propose solutions to address this problem.

We proceed through steps to monitor the machine under an operating condition and collect vibrational data. The machine is. in operating condition. monitored at different dates and vibrational data is collected during the operating condition.

In recent years. engineers have focused on vibration problems of industrial machines and they studied the isolation or the reduction of the vibration. The deterioration of these machines leads to their unavailability. resulting in a loss of production. costs of major maintenance. noise. and vibration. Therefore. it is more critical than necessary for their monitoring and diagnostics. Vibration analysis of rotating machines can better perceive the dynamic phenomena. Vibration measurements and analysis of the signal do not require stopping the engine.

In their work, Boulenger and Pachaud [1] describe the techniques for monitoring and diagnosing machines by vibration analysis, as well as their implementation. The authors analyze the performance and shortcomings of current investigation tools, and the causes of failure in their implementation and give the elements that lead to the success of a reliable monitoring and maintenance policy.

The same Pachaud and Boulenger [2] presents the fundamental principles of the vibration analysis such as nature of the vibrations and the associated quantities, signal processing and acquisition time, the surveillance strategies and vibration images of the ten main faults detected on a rotating machine.

Matsushita et al. [3] explain various phenomena and mechanisms that induce vibrations in rotating machinery, based on theory and field experiences. They also guide undertaking diagnosis and implementing effective countermeasures against various vibration problems in the field.

Aimed at the vibration of the whole aero-engine. Wang et al. [4] build a coupled dynamic model of the rotor-ball bearing-stator of the aero-engine. Taking advantage of the parameters of the signal in the time domain and frequency domain. Frequency characteristics are extracted as the fault features. By the methods of spectrum and cepstrum analysis, the rub-impact characteristics of the casing vibration acceleration time series data are analysed.

The design of a scaled test bench including its main subsystem components at the initial stage is presented by Esteban et al. [5] for the assessment of new methods dedicated to electrical and mechanical faults detection and diagnosis in electromechanical systems.

A MATLAB-based fault diagnosis for sugar industry machines is realised by Joshi et al. [6]. The vibration behaviour of physical industrial machines is obtained, and the signals are provided to a MATLAB program to identify the fault.

Zhai et al. [7] established for practical aero-engine a dual-rotor system multi-body dynamic model with rubbing coupling faults. They introduced a rubbing fault simulation method and they consider a coupling effect between the internal and external rotor. Finally, they compared simulation results with the measured vibration of a dual rotor tester with a rubbing fault.

Jarir and Remond's [8] study deals with the definition of preventive maintenance procedures for gearboxes. Only gear faults are considered. They presented a study of the basic relationship between the presence of gear fault and the modification in the transmission error. Trends of the system response concerning fault evolution were established. Basic relationships between gear failure and the change of transmission error have been discussed.

Boumahdi et al. [9] presented a methodology for the extraction of expert rules in the identification of bearing defects in rotating machinery. Data sets are collected from signals measured by piezoelectric accelerometer fixed on bearings of an experimental set-up.

A peripheral threshold is proposed by Bouzouidja et Al [10] in their classifier to diagnose the new health states of the machines. To verify the effectiveness of the methodology, current, voltage and vibration data from a gearbox system are collected under variable speed and load levels.

In Their paper Joshi et al. [11] deals with a review of the state of the art of vibration condition monitoring and prognosis techniques applied to the rotating machines in sugar industries. It also focuses on case studies of fault diagnosis and rectification of few rotating machines in this industry.

Bearings are the most fragile components of rotating machines. To avoid unforeseen stoppages and costly production. it is then necessary to constantly monitor the condition of the bearings. and monitor the signs of defects: unusual noise. abnormal vibration. overheating. etc. Bourdim el al. [12] studied an approach that shows the influence of the operating conditions of a rolling mill on its lifespan.

Raghav et al. [13] used a Time-domain condition indicators, including kurtosis and skewness, to diagnose the fault in a bevel gear. They present a comparative study of healthy and faulty bevel gear. They observed that condition indicators can identify the existence of a fault in bevel gear.

When it is critical to integrate vibration analysis and wear particle analysis to provide a more effective maintenance program. Huang et al. [14] presented in their work a new fault diagnosis approach for rolling bearings via the combination of vibration analysis and wear particle.

Extensive studies have been conducted by Huang et al. [15] to solve the problem of fault diagnosis under polytropic working conditions (PWC). A novel multisource dense adaptation adversarial network is proposed, which leverages multisensory vibration information and classification label information.

The bearing faults induced in rotating machinery are investigated by Khadersab and Shivakumar [16] experimentally using various vibration analysis techniques that are time, frequency and time-frequency domains.

The study of the dynamic behaviour of a primary jaw crusher showing cracks and deformations in the structure and on the flywheel is discussed by Ouali and Magraoui [17]. Part of the system is treated: the eccentric shaft, connecting rod and movable jaw assembly, as well as the driving pulley and the flywheel. The comparison of the results of the numerical simulation obtained with those found experimentally makes it possible to conclude the appearance of a resonance of the structure by causing cracking and deformations.

In order to proceed with the application of vibration analysis both theoretically and experimentally, a practical case is presented by Magraoui et al. [18]: filtering equipment, the machine has several mechanical faults. To solve these problems. the following solutions are proposed: - Increase the section of the shaft at the level of the rolling bearing that is to say at the places bearing. - Change of bearings - Increase the length of the shaft to facilitate assembly and disassembly of bearings and bearings.

Mohammed Ouali and R. Magraoui [18,19] analyse mechanical failures in rotating machines and carry out their studies while insisting on vibration analysis.

1.1. Case study: DHB decorticator

In this section of the work, a practical case encountered in a semolina mill in Algeria is presented. A DHB wheat decorticator in an industrial semolina mill in the Mill Preparation Zone is shown in (Fig. 1). The numbers 1–4 in Fig. 1 show the different positions of the rotation bearings.

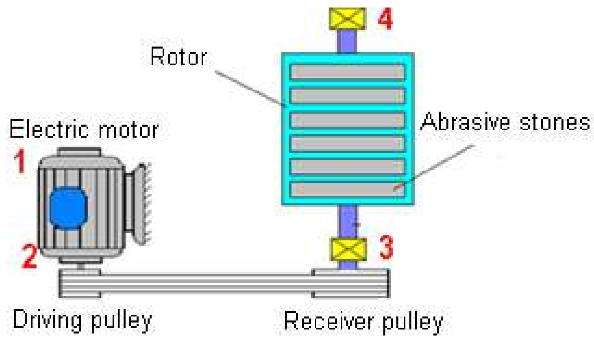

Fig. 1 Schematic of the kinematic chain

2. Semolina Decorticator DHB

2.1. Machine description

The DHB decorticator is a strategic equipment in an industrial semolina mill. Located in the Mill Zone. Its role is to grind wheat particles using abrasive stones mounted in a column, as shown in Figs. 2-5. The setup consists of an electric motor with a power of 55 kW, operating at 1485 rpm, driving a vertical shaft on which seven abrasive stones are mounted. These stones have a diameter of 420 mm and a width of 100 mm (Fig. 4).

Figs. 2 to 5 show abrasive stones configuration.

Fig. 2 Assembly view

Fig. 3 Shaft and stones (first view)

Fig. 4 Shaft and stones (second view)

Fig. 5 Abrasive stones

2.2. Selection of vibration measurement points

The vibration measurement points are chosen precisely to obtain the required information, these points are represented by numbers 1 to 4 in (Fig. 1). In this case, our objective is to understand the overall condition of the machine. Therefore, it is essential to assess the condition of the system's bearings and the behavior of the vertical shaft carrying the abrasive stones under study. Fig. 2 allows for the examination of the machine and the selection of vibration measurement points on the bearings. which will be used to detect any failures that may occur during machine operation. The programming of the measurement points is established in a way that captures all frequencies of interest and monitors their variations in the three directions: horizontal, vertical and axial.

2.3. Vibrational behaviour equations of mechanical system [18, 19]

Consider a system of roller bearings supporting a vertical rotor with a diameter of 100 mm and a length of 1455 mm. upon which the abrasive stones of the Decorticators (Fig. 2 to 4) with a total mass of 959 kg are mounted.

The machine is mounted on a concrete platform. The operational frequency of the machine is 21.25 Hz. The vibration amplitude at this frequency reaches 26.15 mm/s in terms of velocity, according to experimental results from spectral diagnostics. We consider the model represented in Fig. 7. The differential equations of motion are:

$$[M]\{q''(t)\}+[C]\{q'(t)\}+[K]\{q(t)\}=\{F(t)\}, \quad (1)$$

Fig. 6 Operation of vibration measurement sampling on the DHB decorticator

where $[C]$ and $[K]$ are respectively represent the damping matrix and the stiffness matrix, while $[M]$ is typically represents the mass matrix in equations of motion, $\{q''(t)\}$, $\{q'(t)\}$ and $\{q(t)\}$ respectively represent the vectors of generalized accelerations, generalized velocities and generalized displacements as functions of time. $\{F(t)\}$ is vector of generalized forces as a function of time.

3. Vibrations of the Undamped Free System

In the undamped free motion where $[C] = 0$ and $\{F(t)\} = 0$. Then Eq. (1) takes the following form:

$$[M]\{q''(t)\}+[K]\{q(t)\}=0\,. \quad (2)$$

After theoretical study, we arrive at the system of characteristic equations or eigenvalue equations λ:

$$\det\left([K]+S^2[M]\right)=\det\left([K]-\lambda[M]\right)=0\,. \quad (3)$$

3.1. System modelling

The transmission shaft consists of a shaft carrying a receiving pulley and the Decorticator rotor upon which seven identical abrasive stones with a total mass $m = 959$ kg is mounted. The system is supported by two upper and lower bearing housings. In a first approach, the system can be modeled as follows.

A fixing at the level of the receiving pulley. Seven

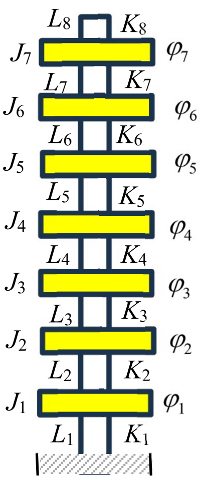

Fig. 7 Theoretical model of the system

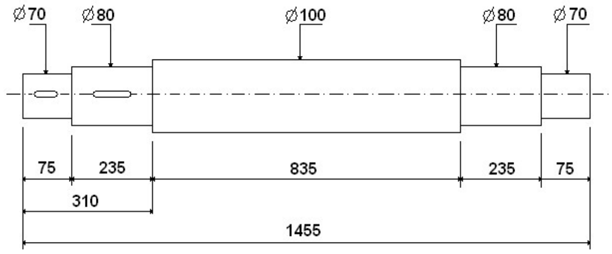

Fig. 8 DHB Decorticator shaft

discs of moments of inertia J_i, where i is from 1 to 7 relating to the abrasive stones mounted on the Decorticator rotor. Each abrasive stone has an outer diameter of d = 420 mm and a mass of $m/7$ = 137 kg.

The shaft is characterized by its stiffnesses K_i (i = 1 … 8) for the 8 sections of the shaft (Fig. 7) as well as its angular deformations from φ_1 to φ_7.

The equivalent system will be approximated to a seven-degree-of-freedom model (Fig. 7). After calculation, the following system of equations is obtained:

$$[J]\cdot\{\ddot{\varphi}\}+[K]\cdot\{\ddot{\varphi}\}=0\,. \tag{4}$$

For the inertia matrix $[J]$ we obtain:

$$[J]=\begin{bmatrix} 2.8496 & 0 & 0 & 0 & 0 & 0 & 0 \\ & 2.8496 & 0 & 0 & 0 & 0 & 0 \\ & & 2.8496 & 0 & 0 & 0 & 0 \\ & & & 2.8496 & 0 & 0 & 0 \\ & Sym & & & 2.8496 & 0 & 0 \\ & & & & & 2.8496 & 0 \\ & & & & & & 2.8496 \end{bmatrix}. \tag{5}$$

For the stiffness matrix $[K]$, considering the model in Fig. 8, we arrive at the determination of K_i, with i = 1 … 8:

$$K_1 = K_8\ 885.907\cdot10^3\ \text{N/m}, \tag{6}$$

$$K_2 = K_3 = K_4 = K_5 = K_6 = K_7 = 5640.705\cdot10^3\ \text{N/m}. \tag{7}$$

After various calculations, the results obtained for the eigenvalues $[\lambda]$, the natural frequencies of the system and the eigenfrequencies are summarized in Table 1.

Table 1
Eigenvalues $[\lambda]$, natural frequencies and eigenfrequencies of the system

N° of the natural frequency	The eigenvalue λ	The natural frequency ω, rad/s	The natural frequency f, Hz
1	$0.0795\cdot10^6$	281.957	44.8631
2	$0.5531\cdot10^6$	743.707	118.3615
3	$1.6394\cdot10^6$	1280.391	203.7817
4	$3.1923\cdot10^6$	1786.701	284.3622
5	$4.9131\cdot10^6$	2216.551	352.7757
6	$6.4629\cdot10^6$	2542.223	404.6068
7	$7.5352\cdot10^6$	2745.032	436.8854

Theoretical natural frequencies of the system are classified in the medium frequency domain. These values will be compared with those determined by numerical simulation and those from experimental study.

4. Experimental Study

4.1. Machine history

Vibration analysis monitoring of the machine began on July 8th/2013. Spectral interpretation revealed the presence of a slight imbalance on the rotor carrying abrasive stones, generating vibrations at a global level of 5.15 mm/s on the engine bearing in the vertical direction (Table 4), deemed acceptable according to international standards VDI 2056. During the vibration monitoring of this equipment (trend curves in Fig. 9 and 10). vibration analysis led us to conclude the existence of an imbalance on the rotor carrying abrasive stones and bearing defects in both bearings supporting the decorticator rotor.

Nevertheless. it is worth noting that during the machine's operation, alarming and dangerous vibration levels were recorded, especially on October 16th/2018. January 20th/2020. October 14th/2020 and November 10th/2021. where the global vibration levels were 8.68 mm/s, 9.86 mm/s, 7.47 mm/s and 8.02 mm/s, respectively. These vibration levels are considered alarming according to international standards VDI 2056, except for the measurement on April 14th/2021. where the recorded global level exhibited an upward trend of 18,74 mm/s, deemed dangerous according to the aforementioned international standards.

Interventions, including the replacement of abrasive stones due to wear, as indicated in Table 1, led to bearing defects in both upper and lower bearings supporting the

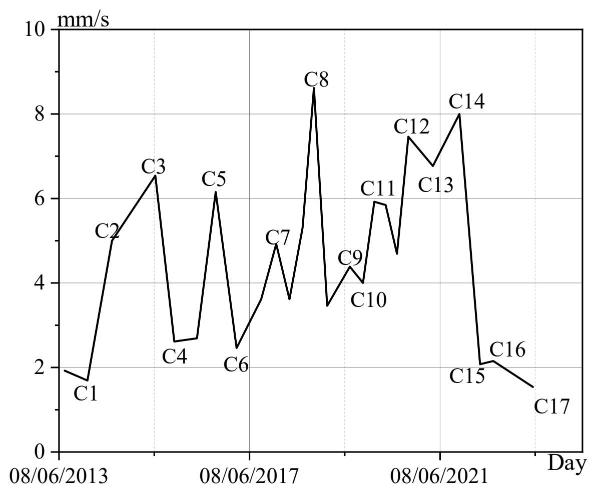

Fig. 9 Trend curve taken on the motor bearing of the decorticator in the horizontal direction

Table 2

Values of specific points in Fig. 9

	Date	mm/s		Date	mm/s
C1	08/07/2013	01.95	C14	10/11/2021	08.02
C3	10/06/2015	06.59	C16	20/07/2022	02.18
C5	27/09/2016	06.27	C17	21/05/2023	01.53
C8	16/10/2018	08.68	-	-	-

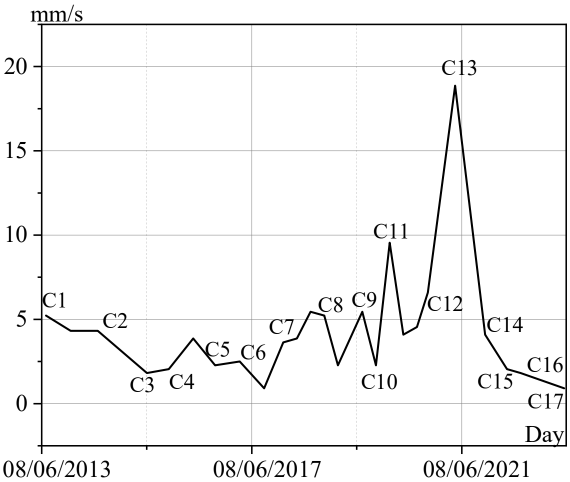

Fig. 10 Trend curve taken on the motor bearing of the decorticator in the vertical direction

Table 3

Values of specific points in Fig. 10

	Date	mm/s		Date	mm/s
C1	08/07/2013	05.15	C14	10/11/2021	04.23
C3	10/06/2015	01.77	C16	20/07/2022	01.86
C11	20/01/2020	09.86	C17	21/05/2023	0.7756
C13	14/04/2021	18.74	-	-	-

decorticator rotor, ultimately resulting in the shearing of the shaft carrying the decorticator. Bearing replacements and rotor balancing were carried out on July 18th/2019. April 14th/2021. and October 10th/2021. Currently. the machine is operating without vibration constraints.

Note: In the graphs (Fig. 9 and 10), the various C_i (i = 1 to 17) represent the overall levels of vibration speeds considered important. The latter are taken at points 02 RH and 02 RV respectively in the radial horizontal and radial vertical direction, on different dates.

In the tables 2 and 3 some values of vibration levels taken from Fig. 9 and 10 respectively are listed.

4.2. Vibration diagnosis and analysis of results

The spectral analysis of the measurements taken on the entire kinematic chain of the machine has allowed us to conclude the presence of the following anomalies.

- June 10th/2015: The appearance of an imbalance defect on the rotor carrying the abrasive stones of the decorticator, generating vibrations at a level of 7.49 mm/s, as indicated by the predominant component related to the rotation frequency of 21.25 Hz, represented in the spectrum of the 500 Hz band Fig. 11, taken on motor bearing No. 2 in the horizontal direction. This imbalance defect manifests slightly on the same bearing but in the vertical direction, generating vibrations at a level of 2.36 mm/s, as indicated by the peak of the predominant component related to the rotation frequency of 20 Hz, represented in the spectrum of the 1000 Hz band (Fig. 12). These two recorded vibration levels are considered respectively alarming and acceptable according to the criteria for judging vibrations, based on the international standards VDI 2056.

Table 4

Summary of vibration measurements and interventions carried out

Date of measurement	Overall vibration level in mm/s on bearing No. 02 in the horizontal direction	Overall vibration level in mm/s on bearing No. 02 in the vertical direction	Comments
08/07/2013	01.95	02.15	
03/07/2014	04.95	04.36	
10/06/2015	06.59	01.77	Wear of abrasive stones
05/11/2015	02.63	01.95	
27/09/2016	06.27	02.25	Chagang abrasive stones.
08/03/2017	02.46	02.54	
06/01/2018	04.96	03.66	
16/10/2018	08.68	05.09	Deterioration of only one abrasive stone. the one at the bottom.
18/07/2019	04.42	05.50	Replacing the two bearings supporting the rotor.
21/10/2019	03.98	02.29	
20/01/2020	05.95	09.86	Wear of the abrasive stones.
14/10/2020	07.47	06.53	
14/04/2021	06.77	18.74	Replacement of the abrasive stones. correction of the bearing seats. and balancing of the rotor.
10/11/2021	08,02	04,23	Replacement of the two bearings supporting the rotor.
18/04/2022	02.03	01.97	
20/07/2022	02.18	01.86	
21/05/2023	01.53	0.7756	

This unbalance problem is due to the beginning of wear on the abrasive stones mounted on the vertical rotor of the machine (Fig. 5). The work carried out: replacement of the abrasive stones.

- April 14th/2021: Detection of an imbalance on the decorticator's rotor, generating vibrations at a level of 14.06 mm/s at the rotation frequency of 20 Hz corresponding to the rotational speed of 1200 rpm, deemed Dangerous according to the international standard VDI 2056, as indicated by the predominant component related to the base frequency of 20 Hz (Fig. 13). This fault still causes vibrations

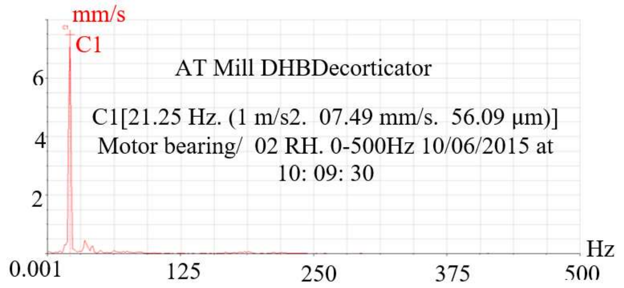

Fig. 11 Spectrum taken on motor bearing N°2 in the horizontal direction, on June 10th 2015

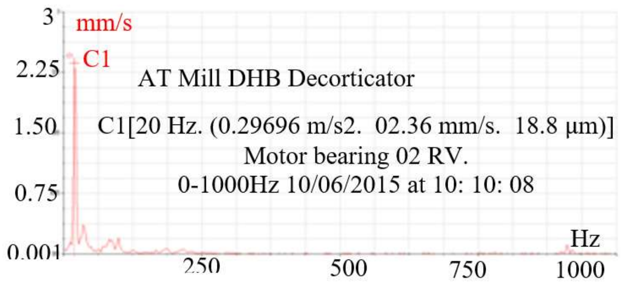

Fig. 12 Spectrum taken on motor bearing N°2 in the vertical direction on June 10th 2015

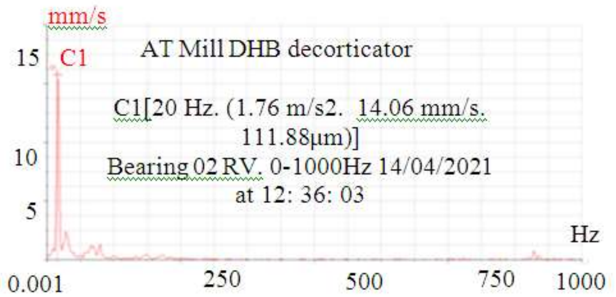

Fig. 13 Spectrum taken on motor bearing No 2 in the vertical direction on April 14th 2021

of a level of 06,35 mm/s in the horizontal direction of the same bearing, as indicated by the preponderant component related to the rotation frequency of 21.25 Hz (Fig. 14). This imbalance is caused by the significant wear of the abrasive stones. resulting in play on the bearing seat in both bearings supporting the decorticator. as indicated by the impact related to the comb of streaks (Fig. 15). taken on the aforementioned bearing in the horizontal direction. in the form of harmonies at the dominant frequency of 20 Hz.

The work carried out:

- loading and machining of the bearing seats on the shaft of the decorticator;
- repair of the two bearings supporting the decorticator's rotor;
- replacement of bearings with reference 22216 CCK C3 in the two aforementioned bearings;
- manufacturing and replacement of the upper and lower hoops;
- balancing of the decorticator's rotor;
- replacement of the abrasive stones.

• July 20th/2022: The spectral interpretation of vibration measurements taken on engine bearing No. 2 reveals the presence of a slight imbalance in the early state of the decorticator rotor, generating slight vibrations at a level of

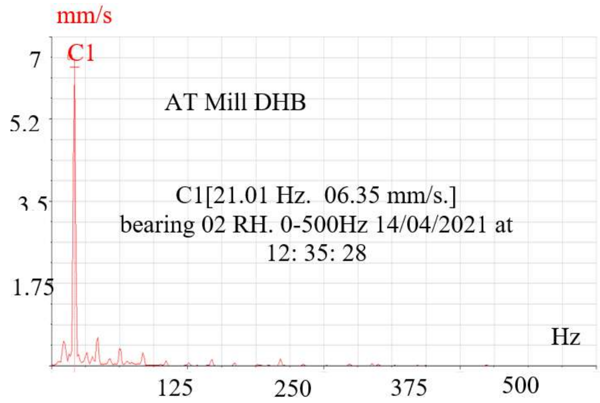

Fig. 14 Linear mode spectrum taken on motor bearing No 2 in the horizontal direction on April 14th 2021

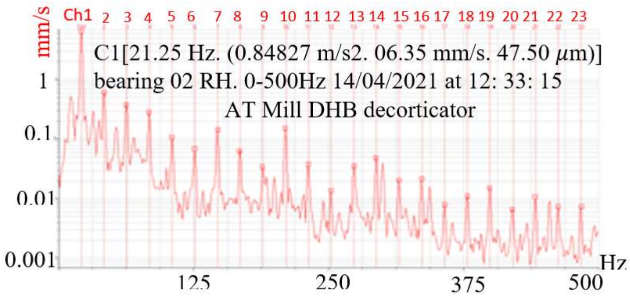

Fig. 15 Logarithmic mode spectrum taken on motor bearing No 2 in the horizontal direction on April 14th 2021

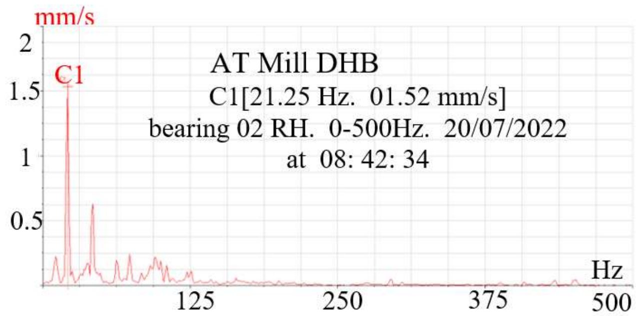

Fig. 16 Spectrum taken on motor bearing N°. 2 in the horizontal direction

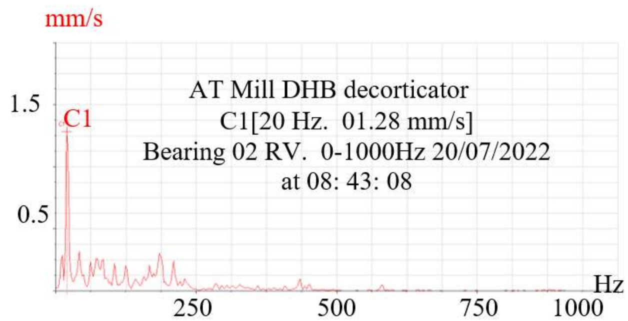

Fig. 17 Spectrum taken on motor bearing N° 2. in the vertical direction

01.52 mm/s. This is indicated by the predominant component related to the rotation frequency of 21.25 Hz. as shown in the 500 Hz band spectrum (Fig. 16). In the vertical direction, the vibration level caused by this imbalance is 01.28 mm/s, according to the predominant frequency of 20 Hz, represented in the 1000 Hz band spectrum (Fig. 17). These two recorded vibration levels are considered good (VDI 2056).

The results obtained during the vibrational diagnosis of the machine have been summarized in the Table 5. These recorded experimental results will be compared with those found theoretically and numerically.

Table 5
Results of frequencies of machine components experimentally detected in practice.

Machine components	Electric motor	Belts	Shaft carrying the decorticator	Comment
Frequency and defect related to the component in Hz.	24.75 Hz 49.50 Hz. 74.25 Hz. 99 Hz. 123.75 Hz. 148.50 Hz. 173.25 Hz. 198 Hz. 222.75 Hz Harmonic frequencies multiples of the fundamental frequency.	10.93 Hz Belt passing frequency	21.25 Hz. 42.50 Hz. 63.75 Hz. 85 Hz. 106.25 Hz. 127.50 Hz. 148.75 Hz. 170 Hz. 191.25 Hz Harmonic frequencies multiples of the fundamental frequency.	The detected harmonic frequencies are related to the wear of the component in question. The base frequency represents the imbalance of the component.

5. Numerical Simulation of the Decorticator Rotor

5.1. Numerical simulation of the decorticator rotor using SolidWorks software

5.1.1. System modelling

This part of the study allows us to establish a numerical modal analysis of the system. Through the design and numerical simulation of the system using SolidWorks, we determined the modes and natural frequencies of the system. The simulation is performed on the empty rotor without abrasive stones (Fig. 18). and then with abrasive stones (Fig. 19).

The rotor carrying the decorticator consists of a shaft with three different sections: diameters of 70 mm. 80 mm. and 100 mm. It is made of stainless steel with a length of 1455 mm. The abrasive stones are mounted along the length of the shaft with a diameter of 100 mm.

The receiving pulley is made of cast iron with a diameter of 250 mm. There are seven abrasive stones. each with an outer diameter of 420 mm, carried over a length of 835 mm. The total mass of the stones is 959 kg, and the limit conditions are rotational guidance at the bearings seen in Fig. 20. The meshing is illustrated in Fig. 21.

5.1.2. Result of the system simulation

The results of the numerical simulation by SolidWorks (modal analysis) have been summarized in the Table 6.

It should be noted that we have considered only torsional vibration modes in order to compare them with those found by the theory (theoretical model established based on torsional vibrations).

The mode shapes of the system are shown in Figs. 22-28.

Fig. 18 Modelling of the system without abrasive stones by SolidWorks

Fig. 19 Modelling the decorticator with abrasive stones using SolidWorks

Fig. 20 Modelling and fixation conditions of the decorticator model

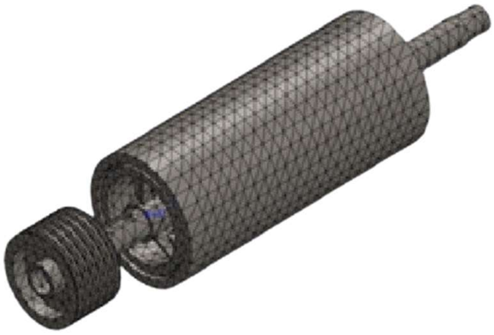

Fig. 21 Meshing of the decorticator model established by SolidWorks

Table 6

List of natural frequencies of the system

mode N°	Natural frequency, Rad/s	Natural frequency, Hz
1	219.13	34.876
2	646.77	102.937
3	1 385.1	220.443
4	1 568.2	249.589
5	2 403.8	382.582
6	2 871.9	457.079
7	2 885.8	459.289

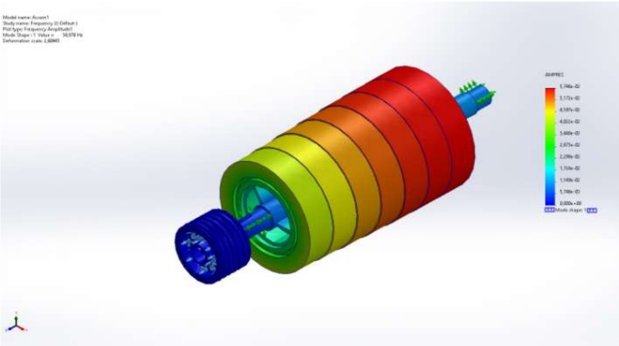

Fig 22 First vibration mode at a frequency of 34.876 Hz

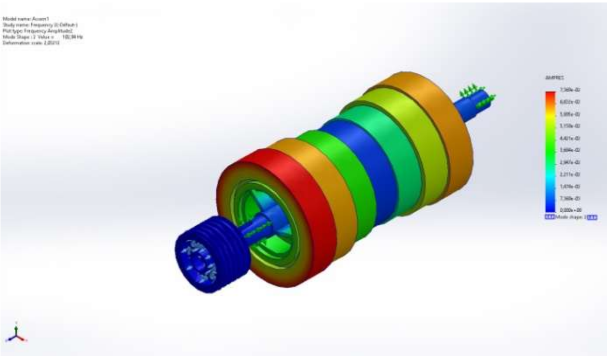

Fig. 23 Second vibration mode at 102.937 Hz frequency

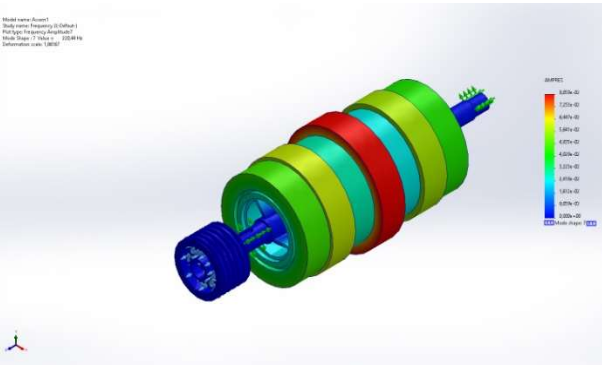

Fig. 24 Third vibration mode at 220.443 Hz frequency

5.2. Numerical simulation of the decorticator rotor using ANSYS software

The results of the numerical simulation using ANSYS modal analysis of the decorticator have been summarized in the Table 7.

We considered only torsional vibration modes in order to compare them with theoretically determined ones. It is worth recalling that we established the theoretical model. considering only torsional vibrations.

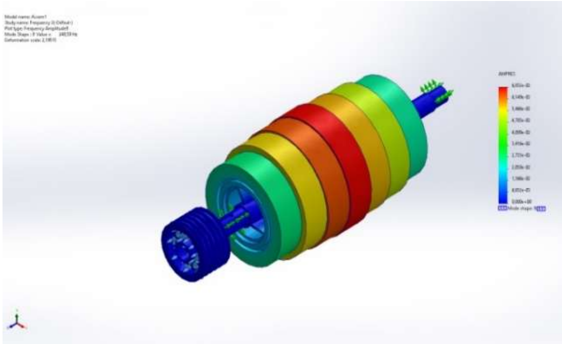

Fig. 25 Fourth vibration mode at a frequency of 249.589 Hz

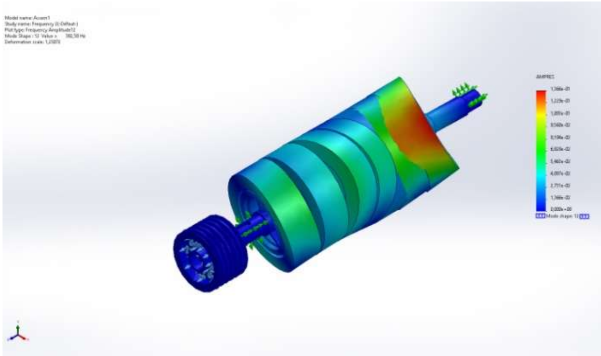

Fig. 26 Fifth vibration mode at a frequency of 382.582 Hz

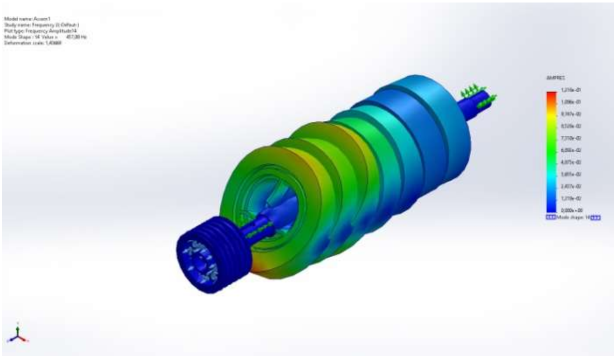

Fig. 27 Sixth vibration mode at 457.079 Hz frequency

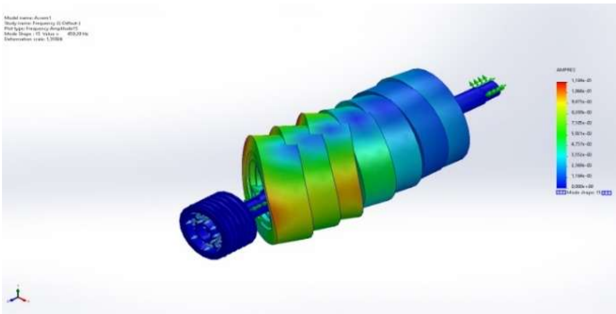

Fig. 28 Seventh vibration mode at 459.289 Hz frequency

Table 7

Result of modal analysis by ANSYS

mode No	Natural frequency, Rad/s	Natural frequency, Hz
1	301.21	47.963
2	646.90	103.01
3	1 362.4	216.94
4	1 414	225.16
5	2 173.9	346.17
6	2 709.3	431.41
7	2 712.8	431.97

The modal deformations of the system are depicted in Figs. 29-35.

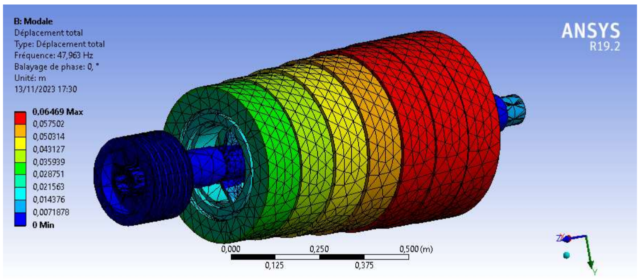

Fig. 29 First vibration mode at a frequency of 47.963 Hz

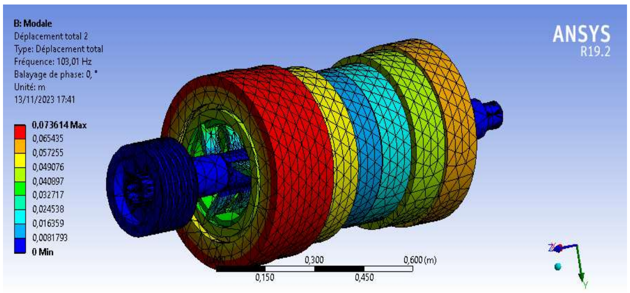

Fig. 30 Second vibration mode at a frequency of 103.01 Hz

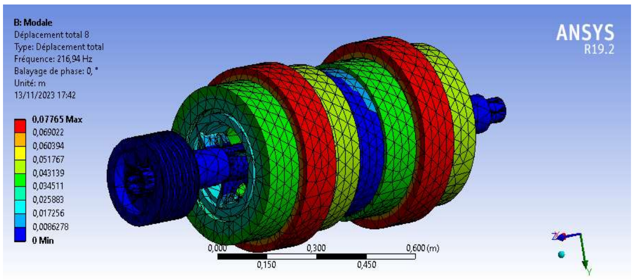

Fig. 31 Third vibration mode at a frequency of 216.94 Hz

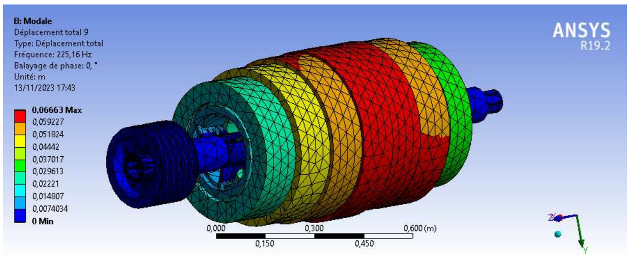

Fig. 32 Fourth vibration mode at a frequency of 225.16 Hz

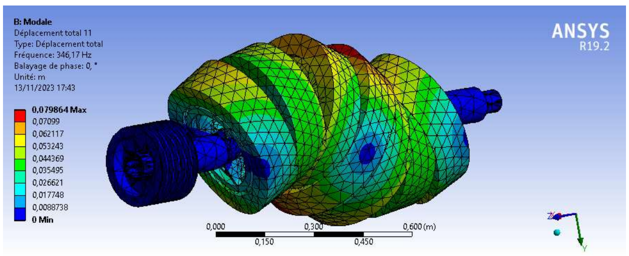

Fig. 33 Fifth vibration mode at a frequency of 346.17 Hz

6. Confrontation of Numerical and Experimental Results

The mechanical faults detected during the operation of the machine are primarily imbalance on its rotor

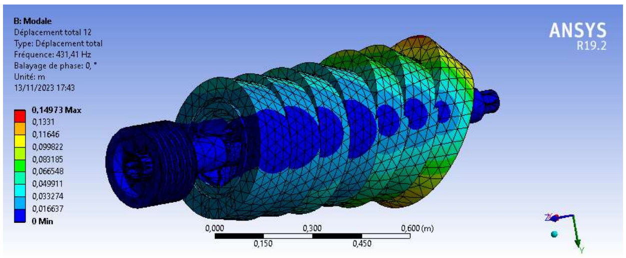

Fig. 34 Sixth vibration mode at a frequency of 431.41 Hz

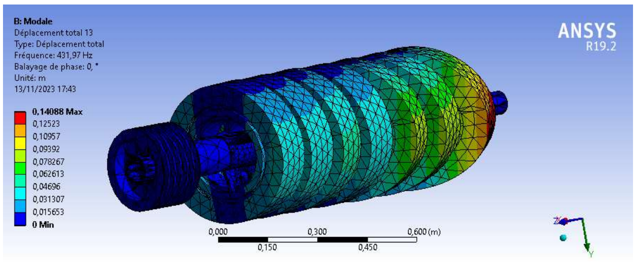

Fig. 35 Seventh vibration mode at a frequency of 431.97 Hz

causing play on the bearing supports carrying this rotor. This play is interpreted by the presence of harmonics, in the form of a component at the base frequency of 21.25 Hz (see Fig. 15), which corresponds to the rotation speed of the decorticator's rotor. Mechanical or electrical faults related to the base frequency of 24.75 Hz, corresponding to the rotation speed of the electric motor at 1485 rpm, and its harmonics, do not appear in the spectra. These potential faults have not manifested themselves so far. Therefore, we will illustrate these different results in the Table 8.

Comment: The results of the numerical simulation agree with the frequencies detected through experimentation for the seven torsional vibration modes generated by the decorticator. Meanwhile. those of the electric motor coincide in most of the torsional vibration modes.

6.1. Comparison of theoretical results with experimental measurements

According to Tables 4 and 8 we obtain Table 9.

Comment: The comparison of the numerical simulation results shows good agreement with the frequencies detected through experimentation, related to those generated by the decorticator and the electric motor across the seven torsional vibration modes. Natural frequency measurements are also affected by vibrations occurring in other joints of the full dynamic system. This may explain the differences between theoretical and experimental results.

6.2. Comparison and validation of theoretical results with those from numerical simulation

As shown in Table 10, the theoretical results are consistent with those of the numerical simulation. especially in the first, second, third, fifth and seventh modes of torsional vibration.

7. Proposed Solutions

The decorticator presents mechanical failures. namely: the imbalance of the decorticator-carrying rotor and the failures of its bearings. as well as wear in its bearings.

Table 8

Comparison of the results of the numerical simulation with those of the experimental

Eigen frequency number	Determined by SolidWorks, Hz	Determined by ANSYS, Hz	Experimentally detected frequency, Hz	
			The fundamental frequency of the electric motor (24.75)	The fundamental frequency of the decorticator rotor (21.25 Hz)
1	34.8755	47.96	49.50 Hz Second harmonic of the fundamental frequency	42.50 Hz Second harmonic of the fundamental frequency
2	102.937	103.01	99 Hz Fourth harmonic of the fundamental frequency	106.25 Hz The fifth harmonic of the fundamental frequency.
3	220.443	216.94	222.75 HzThe ninth harmonic of the fundamental frequency	212.50 Hz The tenth harmonic of the fundamental frequency.
4	249.589	225.16	222.75 Hz Ninth harmonic of the fundamental frequency 247.5 Hz The tenth harmonic of the fundamental frequency.	255 HzThe twelfth harmonic of the fundamental frequency
5	382.582	346.17	346.5 Hz The fourteenth harmonic of the fundamental frequency.	340 Hz The sixteenth harmonic of the fundamental frequency. 382.5 Hz The eighteenth harmonic of the fundamental frequency
6	457.079	431.41		425 Hz Twentieth harmonic of the fundamental frequency 446.25 Hz Twenty-ninth harmonic
7	459.289	431.97		467.5 Hz The twenty second harmonic of the fundamental frequency

These encountered defects have led to very high-level vibrations deemed. Dangerous according to the international standard VDI 2056. These problems have caused unexpected production stops since its commissioning, due to shearing of the rotor's shafts.

Therefore, we have conducted comprehensive practical vibrational diagnostics enriched by theoretical and numerical studies. Solutions have been proposed to address these issues. These solutions are endorsed by modification work, namely:

Table 9

Theoretical and experimental results

N° of the natural frequency	Theoretically determined.	The frequency detected experimentally in Hertz, Hz	
		The fundamental frequency of the electric motor. (24.75)	The fundamental frequency of the decorticator rotor (21.25)
1	44.8631	49.50 Hz deuxième harmonie de la fréquence de base	42.50 Hz The second harmonic of the fundamental frequency
2	118.3615	123.75 Hz The fifth harmonic of the fundamental frequency	106.25 Hz The fifth harmonic of the fundamental frequency
3	203.7817	198 Hz The eighth harmonic of the fundamental frequency	212.50 Hz The tenth harmonic of the fundamental frequency
4	284.3622	272.25 Hz The eleventh harmonic of the fundamental frequency.	276.25 Hz The thirteenth harmonic of the fundamental frequency
5	352.7757	346.5 Hz The fourteenth harmonic of the fundamental frequency.	340 Hz The sixteenth harmonic of the fundamental frequency
6	404.6068	396 Hz The sixteenth harmonic of the fundamental frequency.	403.75 Hz The nineteenth harmonic of the fundamental frequency.
7	436.8854	445.5 Hz The eighteenth harmonic of the fundamental frequency.	446.25 Hz The twentieth harmonic of the fundamental frequency.

Table 10

Theoretical and numerical simulation results

Eigenfrequency number	Determined theoretically	The frequency determined numerically in Hertz.	
		SolidWorks	ANSYS
1	44.8631	34.8755	47.96
2	118.3615	102.937	103.01
3	203.7817	220.443	216.94
4	284.3622	249.589	225.16
5	352.7757	382.582	346.17
6	404.6068	457.079	431.41
7	436.8854	459.289	431.97

- Increase in the width of both the upper and lower hoops, fixing the abrasive stones in stainless steel by 5 mm each from 11 mm to 16 mm in width (Fig. 18).
- The installation of three gussets in the form of a triangle in the upper and lower part of the decorticator's shaft. These gussets are placed to consolidate the hoop and the shaft of the decorticator in the upper and lower part. (Fig. 36).

Before proceeding with the modification, following the proposed solutions a comprehensive numerical study was conducted.

Fig. 36 Modelling of the modified decorticator without abrasive stones

7.1. Design and simulation of the modified system using SolidWorks without abrasive stones

The modal deformation without abrasive stones is shown in Fig. 37. The mesh is represented in the Fig. 38.

Fig. 37 Deformation of the modified decorticator without abrasive stones

Fig. 38 Meshing on the modified decorticator without abrasive stones

7.2. Results of the simulation by SolidWorks and list of eigenmodes of the modified system at no load

We established the simulation up to ten eigenmodes (Table 11). As an example. we will present the first three eigenmodes and their modal shapes (Figs. 39 to 41).

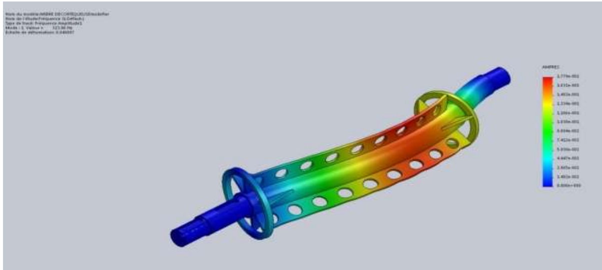

Fig. 39 First vibration mode of the modified system under no load at 323.976 Hz

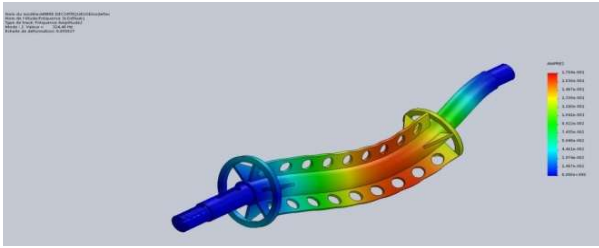

Fig. 40 Second vibration mode of the modified system under no load at 324.476 Hz

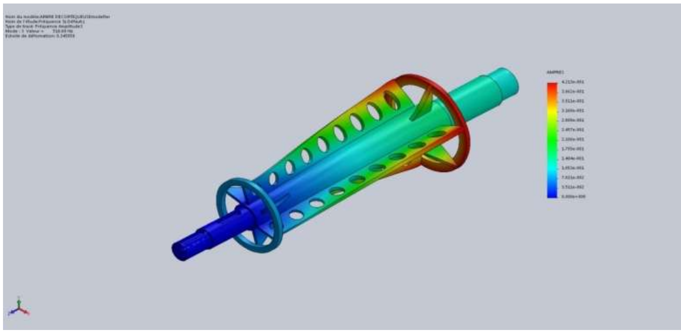

Fig. 41 Third vibration mode of the modified system under no load at 518.087 Hz

Table 11

List of established modes on the modified decorticator without abrasive stones

Frequency No	Rad/sec	Hz	seconds
1	2035.6	323.98	0.0030867
2	2038.7	324.48	0.0030819
3	3255.2	518.09	0.0019302
4	4704.6	748.75	0.0013356
5	5281.6	840.6	0.0011896
6	5288.2	841.64	0.0011882
7	7776.3	1237.6	0.00080799
8	9616.1	1530.4	0.0006534
9	9627.4	1532.2	0.00065264
10	9895.4	1574.9	0.00063496

7.3. Interpretation of the results of the simulation of the decorticator under no load

The results of the numerical simulation using SolidWorks (modal analysis) of the modified rotor under no load have been summarized in Table 11.

The first and second vibration modes represent bending. The third and fourth vibration modes represent the torsional mode. The fifth and sixth modes represent bending modes. The remaining natural modes manifest at high frequencies and represent torsion for the seventh mode, bending for the eighth and ninth vibration modes, and finally, torsion for the tenth vibration mode. It is worth noting that these natural modes are far from coinciding with those determined by experimentation. Therefore. the numerical simulation of the modified system under no load has provided satisfaction.

7.4. Design and simulation of the modified system using SolidWorks with abrasive stones.

The modified system with abrasive stones is depicted in Figs. 42 and 43.

Fig. 42 Modelling of the modified decorticator with abrasive stones

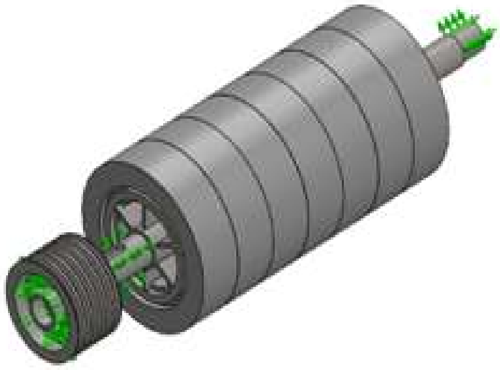

Fig. 43 Fixation conditions of the rotor model for the modified decorticator with abrasive stones

7.5. Results of the simulation by SolidWorks and list of natural modes of the system modified with abrasive stones

The simulation is established in eleven natural modes (Table 12). The modal deformations corresponding to the determined natural modes are presented (Figs. 44-54).

7.6. Interpretation of simulation results of the loaded system with abrasive stones

The results of the numerical simulation using SolidWorks (modal analysis) of the loaded system with abrasive stones have been summarized in the Table 12. The

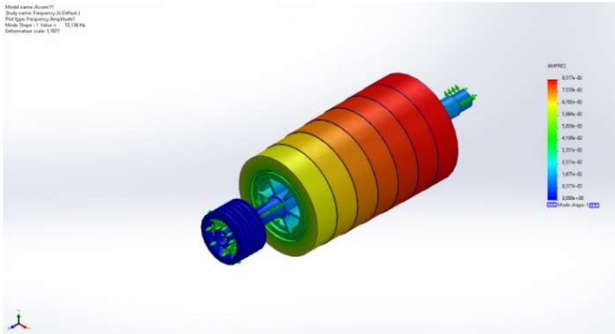

Fig. 44 First vibration mode of the modified system under load at 55.1356 Hz

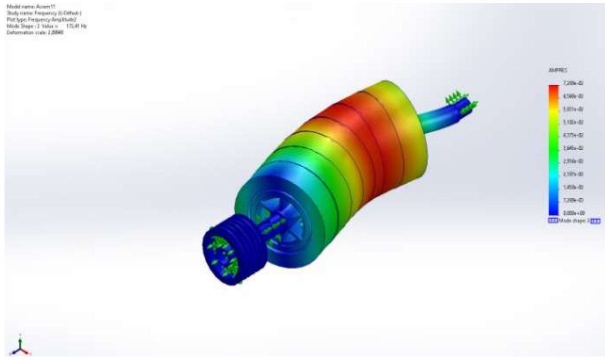

Fig. 45 Second vibration mode of the modified system under load at 172.412 Hz

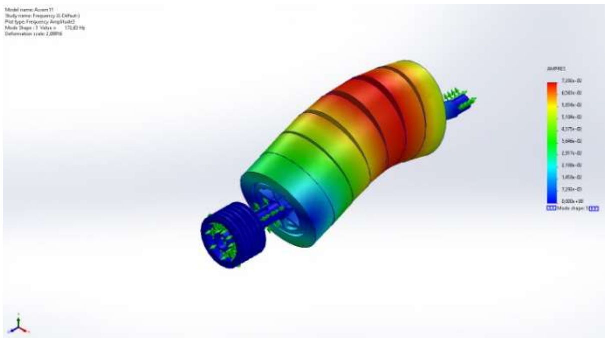

Fig. 46 Third vibration mode of the modified system under load at 172.634 Hz

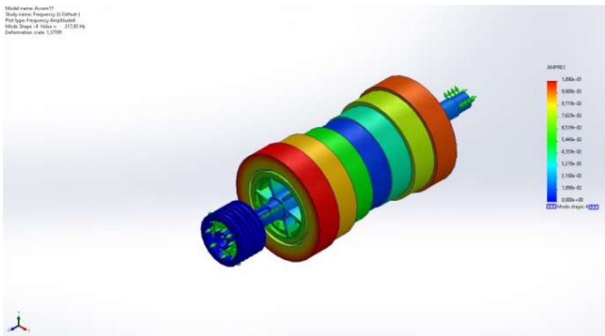

Fig. 47 Fourth vibration mode of the modified system under load at 217.431 Hz

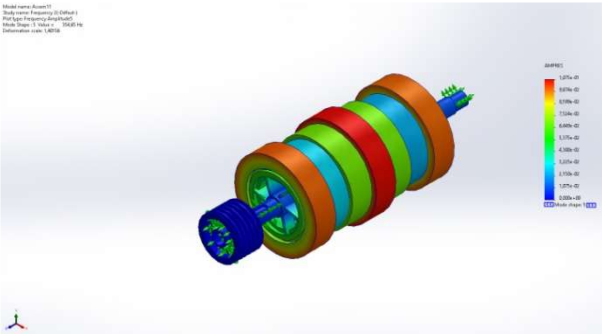

Fig. 48 Fifth vibration mode of the modified system under load at 354.653 Hz

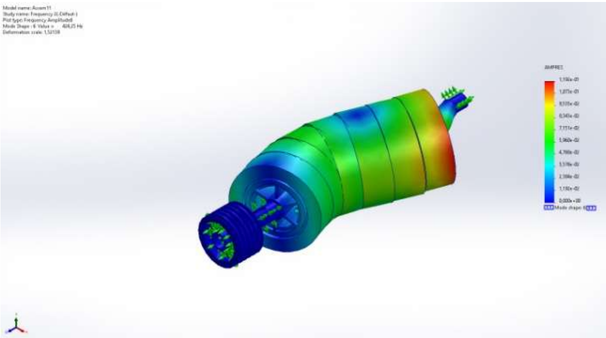

Fig. 49 Sixth vibration mode of the modified system under load at 424.252 Hz

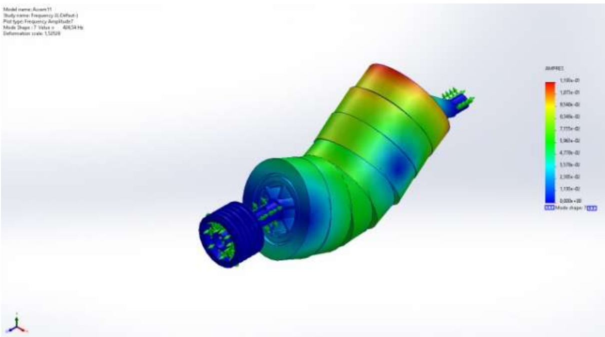

Fig. 50 Seventh vibration mode of the modified system under load at 424.536 Hz

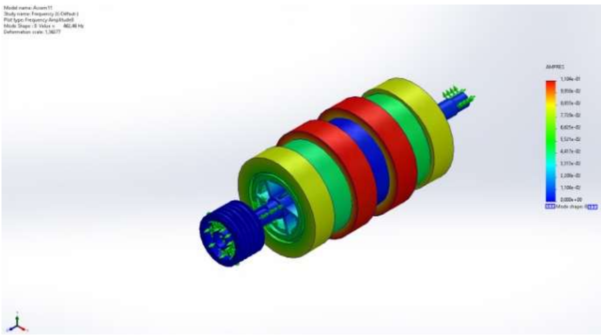

Fig. 51 Eighth vibration mode of the modified system under load at 462.457 Hz

first vibration mode represents the torsional mode, occurring at a frequency of 55.136 Hz. The second and third vibration modes represent the bending mode, occurring at frequencies of 172.41 Hz and 172.63 Hz. respectively. The fourth and fifth vibration modes represent torsion, while the sixth and seventh vibration modes represent bending. The remaining vibration modes all represent torsion.

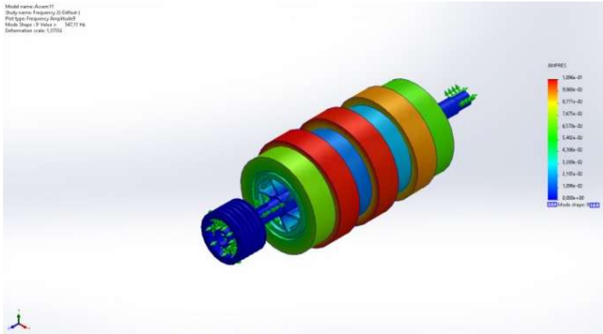

Fig. 52 Ninth vibration mode of the modified system under load at 547.114 Hz

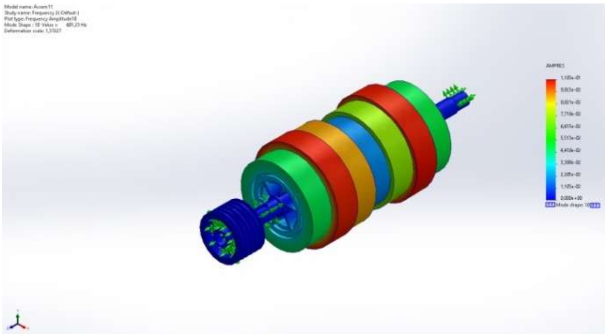

Fig. 53 Tenth vibration mode of the modified system under a load at 601.231 Hz

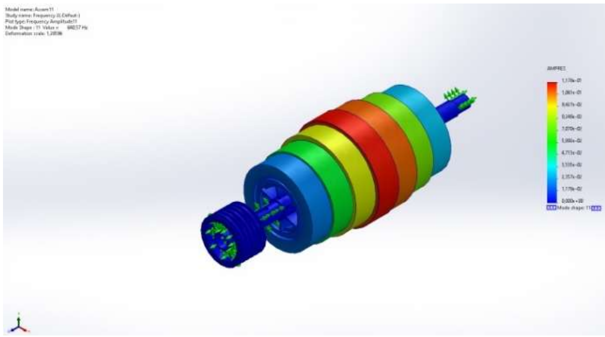

Fig. 54 Eleventh vibration mode of the modified system under a load at 640.572 Hz

Table 12

Established modes for the modified decorticator with abrasive stones

Frequency No	Rad/sec	Hertz	seconds
1	346.43	55.136	0.018137
2	1 083.3	172.41	0.0058001
3	1 084.7	172.63	0.0057926
4	1 366.2	217.43	0.0045992
5	2 228.4	354.65	0.0028197
6	2 665.7	424.25	0.0023571
7	2 667.4	424.54	0.0023555
8	2 905.7	462.46	0.0021624
9	3 437.6	547.11	0.0018278
10	3 777.6	601.23	0.0016633
11	4 024.8	640.57	0.0015611

Based on these results, we observe that the system operates more in torsion than in flexion. Out of the eleven vibration modes, seven modes are torsional with the rest representing only bending modes. The natural frequencies of the modified system have shifted compared to those of the old system (Table 6).

Based on the examination of all these natural modes, we can conclude that the coincidence of these natural frequencies with those of the modified machine in operation under load is far from being achieved. Therefore. we can confirm that the equipment is operating well, away from the phenomenon of resonance.

The modifications were made to the decorticator's rotor. The tests on the modified setup have been made and are yielding satisfactory results.

8. Conclusions

Every rotating machine has moving parts that exert forces on its structure. inevitably causing deformations and resulting in vibrations. These vibrations pose a significant risk to the machine's structures and components, as well as to the environment in which the machine operates. By collecting vibration data through spectral measurements and conducting effective analysis of these measurements, it is possible to determine the source of these vibrations.

In this study, we examined the vibrational behaviour of a critical machine in a semolina mill. Specifically, a DHB semolina decorticator. Since its commissioning, this machine has exhibited mechanical defects such as rotor imbalance, bearing faults. and wear on bearing seats. These failures have led to frequent shutdowns of the installation. disrupting production each time.

By employing vibration analysis techniques using the MOVILOG 2 vibration data collector in conjunction with the DIVADIAG spectral analysis software, we have established reliable and precise vibration diagnostics. As a result, we have not only avoided surprises related to the machine's malfunction but also increased its availability.

The main objective of this work is to validate the theoretical results of proposed modifications aimed at addressing the aforementioned anomalies detected on the decorticator. These modifications involve increasing the thickness of the hoops that hold the abrasive stones in stainless steel material, as well as installing gussets between the shaft and the hoops to reinforce the rotor carrying the abrasive stones of the decorticator.

The theoretical and numerical modal analysis, before and after the proposed modifications, has enabled us to predict the dynamic behaviour of the system, providing a form of assurance for the implementation of these modifications.

The results obtained precisely attest that the theoretical approach and the experimental application converge with acceptable accuracy.

The implementation of the modifications made to the decorticator and their testing have provided complete satisfaction.

References

1. **Boulenger, A.; Pachaud, C.** 2013. Analyse vibratoire en maintenance : surveillance et diagnostic des machines 3e éd. Dunod. 432p.
2. **Pachaud C.; Boulenger, A.** 2009. Aide-mémoire Surveillance des machines par analyse des vibrations. Dunod. 336p.
3. **Matsushita, O.; Tanaka, M.; Kanki, H.; Kobayashi, M.; Keogh., P.** 2017. Introduction of Rotordynamics, in Vibrations of Rotating Machinery. Mathematics for Industry 16. Tokyo: Springer. https://doi.org/10.1007/978-4-431-55456-1_1.
4. **Wang, N, F.; Jiang, D, X.; Han, T.** 2016. Dynamic characteristics of rotor system and rub-impact fault feature research based on casing acceleration, Journal of Vibroengineering 18(3): 1525-1539. https://doi.org/10.21595/jve.2016.16830.
5. **Esteban, E.; Salgado, O.; Iturrospe, A.; Isasa, I.** 2017. Design methodology of a reduced-scale test bench for fault detection and diagnosis, Mechatronics 47: 14-23. https://doi.org/10.1016/j.mechatronics.2017.08.005.
6. **Joshi, M. B.; Pujar, K. S.** 2023. Fault diagnosis of high-speed rotating machines using MATLAB, Diagnostyka 24(2): 2023208. https://doi.org/10.29354/diag/162971.
7. **Ma, P.; Zhai, J.; Zhang, H.; Han, Q.** 2019. Multi-body dynamic simulation and vibration transmission characteristics of dual-rotor system for aeroengine with rubbing coupling faults, Journal of Vibroengineering 21(7): 1875-1887. https://doi.org/10.21595/jve.2019.20206.
8. **Mahfoudh, J.; Remond, D.** 2003. Experimental Study of the Transmission Error for the Detection of Gear Faults. Proceedings of the ASME Turbo Expo 2003, collocated with the 2003 International Joint Power Generation Conference vol. 1: Turbo Expo 2003: 345-349. https://doi.org/10.1115/GT2003-38289.
9. **Boumahdi, M.; Dron, J.P.; Rechak, S.; Cousinard, O**. 2010. On the extraction of rules in the identification of bearing defects in rotating machinery using decision tree, Expert Systems with Applications 37(8): 5887-5894. https://doi.org/10.1016/j.eswa.2010.02.017.
10. **Bouzouidja, M.; Soualhi, M.; Soualhi, A.; Razik, H.** 2024. Detection and Diagnostics of Bearing and Gear Fault under Variable Speed and Load Conditions Using Heterogeneous Signals, Energies 17(3): 643. https://doi.org/10.3390/en17030643.
11. **Joshi, M. B.; Nadakatti, M. M.; Chavan, S. P.;** 2019 Implementation of Diagnostic Technique to Solve Vibration Problems in Sugar Industry: Some Case Studies, International Review of Mechanical Engineering (IREME) 13(6): 318-325. https://doi.org/10.15866/ireme.v13i6.15471.
12. **Bourdim, M.; Bourdim, A.; Kerrouz, S.; Benamar, A.** 2016. Statistical Approach of Bearing Degradation, International Review of Mechanical Engineering (IREME) 10(7): 496-500. https://doi.org/10.15866/ireme.v10i7.9434.
13. **Raghav, M. S.; Tiwari, R.; Sharma, R. B.** 2021. Fault Detection in Bevel Gear Using Condition Indicators. In: Rakesh, P.K.; Sharma, A.K.; Singh. I. (eds) Advances in Engineering Design. Lecture Notes in Mechanical Engineering. Springer. Singapore: 403-416. https://doi.org/10.1007/978-981-33-4018-3_38.
14. **Huang Z, Y.; Yu, Z. Q.; Li, Z. X.; Geng, Y. C**. 2010. A Fault Diagnosis Method of Rolling Bearing through Wear Particle and Vibration Analyses, Applied Mechanics and Materials (26-28): 676-681. https://doi.org/10.4028/www.scientific.net/AMM.26-28.676.

15. **Huang, Z.; Lei, Z.; Wen, G.; Huang, X.; Zhou, H.; Yan, R.; Chen, X.** 2022. A Multisource Dense Adaptation Adversarial Network for Fault Diagnosis of Machinery, IEEE Transactions on Industrial Electronics 69(6): 6298-6307. https://doi.org/10.1109/TIE.2021.3086707.
16. **Khadersab, A.; Shivakumar, S.** 2018. Vibration Analysis Techniques for Rotating Machinery and its effect on Bearing Faults, Procedia Manufacturing 20: 247-252. https://doi.org/10.1016/j.promfg.2018.02.036.
17. **Ouali, M.; Magraoui, R.** 2018. Diagnosis by vibratory analysis of rotating machines. Jaw crusher case. theory and experimentation, International Journal of Mechanical and Production Engineering 6(2): 77-83
18. **Magraoui, R.; Ouali, M.; Temmar, M**. 2018. Vibration Analysis of a Rotating Machine, International Journal of Mechanical and Production Engineering 6(2): 72-76.

R. Magraoui, A. Zemirline, M. Ouali

PREDICTIVE MAINTENANCE OF ROTATING MACHINES, APPLICATION TO THE DHB SEMOLINA DECORTICATOR

S u m m a r y

Real industrial machinery is never perfect. We encounter manufacturing defects, operating clearances, and more effects and parameters: temperature, rotation speeds, etc.

The analysis of vibration is to provide information on the condition of equipment in order to ensure the planning of operations of maintenance.

This study examines condition-monitoring strategies for Semolina Decorticator DH 201.This machine exhibits several simultaneous mechanical faults. including imbalance rupture. bearing defects. and wear. Experimental and numerical results for the detection and identification of numerous faults that may occur in various mechanical components are presented.

To achieve this. various fault indicators are detected or calculated using a vibrational analysis method. We programmed the vibration of measurement points using vibration analysis software. Subsequently. vibration measurements were conducted using a data collector.

The results of theoretical simulations were compared with experimental measurements to determine the severity of mechanical faults and establish an appropriate vibrational prognosis. This work is enriched by the proposed technological solution and potential tests.

Keywords: rotating machinery, decorticator, vibration analysis, unbalance, abrasive stones, damage identification, modelling.

Received March 11, 2024
Accepted October 22, 2025